



Comparison of Surface Ozone Simulation among Selected Regional Models  
in MICS-Asia III  
– Effect of Chemistry and Vertical Transport for the Causes of Difference–

Hajime Akimoto<sup>1</sup>, Tatsuya Nagashima<sup>1</sup>, Li Jie<sup>2</sup>, Joshua Fu<sup>3</sup>, Dongsheng Ji<sup>3</sup>  
and Zifa Wang<sup>2</sup>

1. National Institute for Environmental Studies, Onogawa, Tsukuba 305-8506, Japan
2. Institute of Atmospheric Physics, Chinese Academy of Sciences, Beijing 100029, China
3. Department of Civil and Environmental Engineering, University of Tennessee, Knoxville, TN 37996, U.S.A.

**Abstract**

In order to clarify the cause of variability among the model outputs for surface ozone in the Model Intercomparison Study Asia Phase III (MICS-Asia III), three regional models, CMAQ v.5.0.2, CMAQ v.4.7.1 and NAQPMS (abbreviated as NAQM in this paper) have been selected. The detailed analyses have been made for monthly averaged diurnal variation for select grids covering metropolitan area of Beijing and Tokyo, and at a remote oceanic site, Oki. The chemical reaction mechanism, SAPRC99 used in the CMAQ models tends to give higher net chemical ozone production than CBM-Z used in NAQM agreeing with previous studies. Inclusion of heterogeneous “renoxification” reaction of  $\text{HNO}_3$  (on soot)  $\rightarrow \text{NO} + \text{NO}_2$  only in NAQM is supposed to give higher NO concentration to give better agreement with observational data for NO and nighttime  $\text{O}_3$  mixing ratios. In addition to chemistry, the difference in vertical transport of  $\text{O}_3$  was found to affect the simulated results significantly. Particularly, the increase in downward flux of  $\text{O}_3$  from upper layer to the surface after the dawn is found to be substantially different among the models. Larger early morning vertical transport of  $\text{O}_3$  by CMAQ 5.0.2 would be the reason for higher daytime  $\text{O}_3$  by this model in July. All the three models overestimate the daytime ozone by ca. 20 ppbv at the remote site Oki in July, where in situ photochemical activity is minimal.



## Introduction

In the Model Intercomparison Study Asia Phase III (MICS-Asia Phase III), one of the targets was to narrow down the difference in the model simulation results by using the common key input parameters such as precursor emissions, meteorological fields, and boundary conditions to allow more focused discussion on the causes of the difference among model outputs. In most of the past model intercomparison studies for chemical transport models (CTM) for air quality, such key parameters were not common to all the models, which makes difficult the discussion of the causes of the differences among the model outputs, and the results have often been shown to demonstrate that the ensemble mean of simulated mixing ratios agrees reasonably well with observation even though the disagreement among the models are often significantly large (for example, Han et al., 2008; Fiore et al., 2009).

In order to improve the situation of model intercomparison study, participants of the MICS-Asia III studies agreed to use the common emission data (Li, M. et al., 2017), meteorological field (specified Weather Research and Forecasting Model (WRF)) and the boundary conditions by either of two global CTM (GEOS-Chem and CHASER) provided within the project (Wang et al. overview paper to be submitted; Li, J. et al. in this special issue, to be submitted). The following 12 regional models have been submitted to the MICS-Asia III using the designated common emissions, meteorological field and boundary conditions; six WRF-CMAQ (Community Multiscale Air Quality Modeling System, two v.5.0.2, one v.5.0.1 and three v.4.7.1), four WRF-Chem (Weather Research and Forecasting (WRF) model coupled with Chemistry), one WRF-NHM (JMA NonHydrostatic Model)/Chem and one WRF-NAQPMS (Nested Air Quality Prediction Modeling System, which is abbreviated to NAQM in this paper hereafter for simplicity). It turned out, however, that even though these 12 models uses the common specified key input components, large variability in the spatial distribution and absolute mixing ratios among the models were found for ozone ( $O_3$ ) (Li, J. et al., in this special issue).

In the present study, three regional models, two WRF-CMAQ, v.5.02 and v.4.7.1, and WRF-NAQM were selected among the 12 models to elucidate the causes of difference, and detailed comparison have been made for the selected grids covering metropolitan areas in Beijing and Tokyo, and at a remote oceanic site at Oki in April and July. The reason of the selection of the two models of CMAQ is that CMAQ models have been used widely to assess the air quality for ozone in Asia (e.g. Yamaji et al., 2008; Kurokawa et al., 2009; Fu et al., 2012), and the difference of the simulated results between different version (v. 5.02 and v.4.7.1)



is of concern. The selection of WRF-NAQM is that this is one of the regional CTM developed in Asia, and give substantially lower mixing ratios of surface ozone as compared to the most of WRF-CMAQ including the selected two models (Li, J. et al., in this special issue). The metropolitan areas of two megacities of Beijing and Tokyo have been selected for the comparison because of the concern on the application of the regional models to the mitigation policy of urban ozone pollution. Oki, an EANET (Acid Deposition Monitoring Network in East Asia) monitoring station located in the southern part of the Sea of Japan, is selected as a remote reference site between the two megacities, where in situ photochemical production of  $O_3$  is known to be minimal (Jaffe et al., 1996). April and July have been selected as months for comparison since in situ photochemical production of  $O_3$  is expected to be substantial in July in Beijing and Tokyo, whereas it is thought to be much less in April.

## Models

Basic features and the simulated whole domain of the regional models used in this study, CMAQ v.4.7 (Foley et al., 2010), v.5.0 (CMAS, 2011), and NAQM (Li, J. et al., 2012) are given elsewhere in this issue (Li, J. et al., in this special issue). The employed horizontal resolution is 45 km for all the models, and the highest height and number of vertical layers are 45 km and 40 layers for the CMAQ models and 20 km and 20 layers for the NAQM so that the vertical resolution in the troposphere is about the same. The lowest layer for which the simulated data of ozone were extracted in this paper has the vertical height of ~50 m from the ground. Model calculations by the CMAQ v. 5.0.2, v.4.7.1, and NAQM were conducted at University of Tennessee, National Institute for Environmental Studies, and Institute of Atmospheric Physics, respectively. All the models used the common meteorological fields from WRF (Wang et al., overview paper in this special issue) simulation and common emissions of MIX ( $0.25^\circ \times 0.25^\circ$ ) for 2010 (Li, M. et al., 2017) developed in the MICS-Asia III project. The initial and boundary conditions were supplied by the global models, CHASER for CMAQ v.4.7.1 and NAQM, and GEOS-Chem for CMAQ v.5.0.2. It has been approved that either CHASER or GEOS-Chem may be used in the MICS-Asia III since they were confirmed to give reasonably good agreement for the  $O_3$  field in the Asian domain (Wang et al., overview paper in this special issue).

Other than these three key components (emissions, meteorological field, and boundary conditions), the three models employed different sub-models and parameters for i.e. the gas-phase and aerosol chemistry module, dry deposition parameters, boundary layer scheme, etc.



97 As for the gas-phase chemistry, CMAQ v.4.7.1 and v.5.0.2 incorporated SAPRC99 (Carter,  
98 2000), and NAQM employed CBM-Z (Zaveri and Peters, 1999). In the CMAQ v.4.7.1 (Foley et  
99 al., 2010), major upgrades were made on the aerosol treatment from the previous version of  
100 CMAQ: (a) updates to the heterogeneous  $\text{N}_2\text{O}_5$  parameterization, (b) improvement in the  
101 treatment of secondary organic aerosol (SOA), (c) inclusion of dynamic mass transfer for  
102 coarse-mode aerosol, and (d) revisions to the cloud model. The NAQM and CMAQ v.4.7.1  
103 employed ISORROPIA v.1.7 (Nenes et al, 1998) and CMAQ v.5.0.2 incorporated ISORROPIA  
104 v.2.1 (Fountoukis and Nenes, 2007) for inorganic aerosol chemistry modules. In addition,  
105 CMAQ v.4.7.1 and v.5.0.2 included AERO6 (Binkowski and Rosselle, 2003) as an organic  
106 aerosol chemistry module. As for the advection module, Yamartino (1993), and Walcek and  
107 Aleksic (1998) were used for CMAQ (v.4.7.1 and v.5.0.2) and NAQM, respectively.  
108 Sub-modules for vertical diffusion, dry deposition, and wet deposition employed in the three  
109 models are essentially the same. The Asymmetric Convective Model version 2 (ACM2) for the  
110 planetary boundary layer (PBL) (Pleim, 2007) has been employed both in CMAQ v.4.7.1 and  
111 v.5.0.2. The Yonsei University (YSU) Boundary Layer (BL) scheme is used for calculating BL  
112 height for NAQM (Li, J. et al., 2012).

113

#### 114 **Comparison Domain and Observational Data**

115 All the comparisons among the model simulation and with observational data are made for  
116 monthly averaged diurnal variations for the mixing ratios of  $\text{O}_3$ , and NO in April and July. April  
117 and July are chosen here since in April in situ photochemical buildup of  $\text{O}_3$  is insignificant but  
118 the daytime maximum mixing ratio of  $\text{O}_3$  is relatively high reflecting the well known spring  
119 maximum of  $\text{O}_3$  for the background in the northern hemisphere including East Asia (Monks,  
120 2000; Pochanart et al., 2003), while in July much higher in situ photochemical build up of  $\text{O}_3$  is  
121 expected in urban areas in East Asia. Two representative megacities of Beijing and Tokyo has  
122 been selected as urban areas for the comparison. As a remote reference site, Oki, an EANET site,  
123 was selected between Beijing and Tokyo. Oki site is located on a cliff of an island where the  
124 local emissions of  $\text{NO}_x$  and VOCs are insignificant so that in situ production of  $\text{O}_3$  is also  
125 minimal (Jaffe et al., 1996; Pochanart et al., 2002). Since the NO levels at Oki are too low to get  
126 the meaningful data by the conventional chemiluminescence  $\text{NO}_x$  instrument used for  
127 monitoring, comparison with modeling results are made only for  $\text{O}_3$  at this site. All the  
128 calculations were conducted for a whole year of 2010 using the meteorological field and the  
129 emission data for this year.



130 The domains of Beijing and Tokyo and Oki site are centered at 39.9°N, 116.3°E; 36.0°N,  
131 139.3°E and 36.3°N and 133.1°E, respectively. The selected domains for Beijing and Tokyo  
132 consist of 9 (3×3), and 3 (2+1) grids, respectively, covering the metropolitan areas of the cities  
133 as shown in Fig. 1. Data of a single grid covering the island is used for the Oki site. The  
134 observational data used for Tokyo are 1-hr averaged values in 2010 of the average of 118 (for  
135 O<sub>3</sub>) and 126 (for NO) non-roadside monitoring stations within the selected grid shown in Fig. 1.  
136 The data were obtained from Atmospheric Environment Monitoring Data Files in the  
137 Environmental Information Database stored in the National Institute for Environmental Studies  
138 (NIES), Japan. In Beijing, unfortunately, no routine monitoring data of 1-hr averaged values of  
139 O<sub>3</sub> in 2010 is open to the public. Therefore, the unpublished data obtained at two sites (IAP  
140 tower campus and Yangfang) obtained by IAP, and literature values published in Xu et al.  
141 (2011) and Chen et al. (2015) have been referred in this work. The observational data for Oki is  
142 the 1-hr averaged EANET data in 2010 provided on request by the Network Center, Asia Center  
143 for Air Pollution Research (ACAP) (<http://www.acap.asia>).

Fig. 1

## 145 Results

146 Figures 2(a)-(d) depicts the simulated and observed mixing ratios of the monthly averaged  
147 diurnal variations of the O<sub>3</sub> and NO concentrations in April and July in Beijing, and Fig.  
148 3(a)-(d) shows the similar results in Tokyo. The comparisons of the simulated values by the  
149 CMAQ 5.0.2 and 4.7.1 (hereafter, “v.” for version will be omitted for simplicity) and NAQM,  
150 and are plotted in each figure together with the observational data.

Fig. 2

Fig. 3

151 In Beijing, unfortunately observational data of surface ozone at the routine monitoring  
152 stations by the Beijing municipal government is not available until 2013 (Chen et al., 2015).  
153 The average of two observational data obtained by IAP in 2010 is plotted by the dashed lines  
154 with circles in Figs. 2(a) and (b) for O<sub>3</sub> and in Figs. 2(c) and (d) for NO. Another published  
155 observational data of diurnal variation of O<sub>3</sub> in Beijing in April is available by Xu et al. (2011)  
156 at four sites, two urban (Fengtai and Baolian), one suburban (Shunyi), and one rural  
157 (Shangdianzi) in summer (21 June-12 September, mainly covering July and August) in 2007.  
158 Since the diurnal variation of the urban and suburban sites are consistent, the average of these  
159 three sites are plotted in Fig. 2(b) by a dashed line with triangles. In April in Beijing no monthly  
160 average diurnal variation of O<sub>3</sub> is available in a literature. Chen et al (2015) reported the  
161 monthly averaged daily maximum mixing ratio of O<sub>3</sub> ca. 60 ppbv at an urban site (Dongsi), and  
162 ca. 75 and ca. 65 ppbv at two suburban sites (Daxing and Shunyi) within the selected grids in



163 this study. If we simply take the average of these three values, the daily maximum mixing ratio  
164 is ca. 65 ppbv (not shown in Fig. 2(a)). Only the IAP data are plotted for NO with solid lines in  
165 Fig. 2(c) and (d).

166 As can be seen in Figs. 2(a), (b), and Figs. 3(a), (b), the diurnal pattern of the simulated  
167 surface ozone shows the maximum at late afternoon around 14-16 o'clock of the local time both  
168 in Beijing and Tokyo agreeing well with the observation. The simulated mixing ratios of O<sub>3</sub> by  
169 CMAQ 4.7.1 are the highest, and those by NAQM are the lowest both in Beijing and Tokyo and  
170 in April and July in common. The diurnal variations of O<sub>3</sub> simulated by CMAQ 4.7.1 is in  
171 parallel with NAQM for whole days in all cases, but the predicted mixing ratios by CMAQ  
172 4.7.1 are by ca. 20 ppbv and ca. 40 ppbv higher than NAQM in April and July, respectively,  
173 both in Beijing and Tokyo. The O<sub>3</sub> mixing ratios predicted by CMAQ 5.0.2 has a peculiar  
174 characteristics by season, i.e. the mixing ratio is slightly higher but close to NAQM within 10  
175 ppbv both in Beijing and Tokyo in April, whereas in July the daytime O<sub>3</sub> maximum by CMAQ  
176 5.0.2 is very close to CMAQ 4.7.1, much higher than NAQM. In Tokyo, the simulated mixing  
177 ratios of CMAQ 5.0.2 and NAQM are closer to the observation in April, and NAQM gives  
178 closer matching with observation in July, while CMAQ 4.7.1 overestimates in both months as  
179 shown in Figs. 2 (b) and 3(b). Comparison with the observation will be discussed later including  
180 the uncertainty of the observational data in Beijing.

181 The observed mixing ratios of NO shows a peak value at around 7 am, decreases during  
182 morning followed by a slow decay in the afternoon, and starts to build up during nighttime both  
183 in April and July, and in Beijing and Tokyo. The peak values of mixing ratio in the morning are  
184 ca. 13-14 and 6 ppbv in April and ca. 11 and 5-6 ppbv in July in Beijing and Tokyo,  
185 respectively. The minimum mixing ratios in the evening are ca. 1.7 and 1.4 ppbv in April and  
186 2.3 and 1.3 ppbv in July in Beijing and Tokyo, respectively. Thus, it can be noted that the NO  
187 mixing ratios in Beijing are nearly a double of Tokyo.

188 The simulated mixing ratios of NO are generally in the order of NAQM > CMAQ 5.0.2 >  
189 CMAQ 4.7.1., but are much diverse among the models. In April, CMAQ 5.0.2 gives a morning  
190 peak values of 13-14ppbv and ca. 5 ppbv in Beijing and Tokyo, respectively, which agrees well  
191 with observation. NAQM overpredicts NO missing ratio in April in Beijing but gives reasonable  
192 agreement in Tokyo as shown in Figs 2(c) and 3(c). In contrast, CMAQ 4.7.1 gave a broad  
193 daytime peak of only ca. 2 and ca. 1 ppbv in April in Beijing and Tokyo, respectively, which is  
194 quite different from other models and much underpredicts the observational data. In July, only  
195 NAQM gives a morning peak mixing ratio of ca. 8 and 5.5 ppbv in Beijing and Tokyo agreeing



196 fairly well with the observation including diurnal variation as seen in Figs. 2(d) and 3(d). In  
197 contrast, both CMAQ 5.0.2 and 4.7.1 give a morning peaks as low as 1-2 ppbv and nearly zero  
198 mixing ratio during nighttime, which are significantly lower than the observation.

199 It can be noted that the simulated and observed levels of  $O_3$  is highly anti-correlated with  
200 those of NO. For example, the reasonably good agreements of  $O_3$  by CMAQ 5.0.2 and NAQM  
201 in April, and by NAQM in July in Tokyo correspond to the reasonably good agreement of NO  
202 in each case. Much higher overestimate of  $O_3$  by the CMAQ 4.7.1 in April and by both the  
203 CMAQ 5.0.2 and 4.7.1 in July correspond the substantial underestimate of NO.

204 Figures. 4(a) and (b) shows monthly averaged diurnal variation of  $O_3$  mixing ratios at Oki in  
205 April and July, respectively. As shown in Fig. 4(a), all the three models give consistent mixing  
206 ratios of  $O_3$  at 60-65 ppbv in April, which agree well with observation within 10 ppbv. In July,  
207 although the simulated mixing ratios of  $O_3$  agree well each other within 10 ppbv, they are in the  
208 range of 50-70 ppbv as compared to observational level of 35-45 ppbv. Thus, all the three  
209 models overestimate the  $O_3$  mixing ratio by nearly 20 ppbv. Although the characteristics of  
210 remote sites showing only a slight daytime build up of  $O_3$  is well reproduced by the models,  
211 substantial overestimate of the simulated  $O_3$  mixing ratio compared to the observation should be  
212 of concern in July.

Fig. 4

## 214 Discussion

215 The causes of the differences of the simulated results among the three models mentioned  
216 above must be due to either chemistry or transport processes incorporated in the models. Here,  
217 the possible causes of differences of those processes are discussed individually.

## 218 Comparison of Chemical Mechanism Sub-Modules

219 One of the differences in the three models in this study is the chemical reaction mechanism  
220 sub-module. CMAQ 5.0.2 and 4.7.1 incorporate SAPRC99 while NAQM employs CBM-Z. It  
221 has been well known that different photochemical mechanisms used in the regional chemical  
222 transport models produce dissimilar results on the prediction of  $O_3$ . Jimenez et al. (2003)  
223 compared seven photochemical mechanisms including CBM-IV (Gery et al., 1989) and  
224 SAPRC99 using a box model. Comparison of CBM-IV, CBM-V (Sarwar et al., 2008) and  
225 SAPRC99 incorporated into a regional chemical transport models have been made by Faraji et  
226 al. (2007) and Luecken et al. (2008). The main difference among these mechanisms has been  
227 noted to be the lumping technique describing organic compounds into surrogate groups





228 (Jemenez et al., 2003), the differences in the products of the reaction of aromatics with OH  
229 radical, and the overall branching ratio of radical generation and termination reactions (Faraji et  
230 al., 2007). The results of these studies gave a consistent picture that SAPRC99 gives higher  
231 concentrations of O<sub>3</sub> than CBM-IV both in the box model calculation and regional model  
232 simulation over United States. The O<sub>3</sub> concentration obtained by CBM-V is reported to be in  
233 between the CBM-IV and SAPRC99 (Luecken et al., 2008). The reason for giving the higher  
234 concentration of O<sub>3</sub> by SAPRC99 has been deduced to be due to the more efficient peroxy  
235 radical production in the photochemical reaction scheme of SAPRC99 compared to CBM  
236 modules.

237 Figures 5 (a)-(d) show the net chemical production of O<sub>3</sub> in Beijing and Tokyo in April and  
238 July calculated in this study. As revealed in the figure, CMAQ models give higher net ozone  
239 production than NAQM, which is consistent with the results of earlier studies showing  
240 photochemical reaction scheme of SAPRC99 gives higher O<sub>3</sub> production than CBM modules.  
241 The reaction scheme of CBM-Z is the revision of CBM-IV, and the major revision is described  
242 as (1) including revised inorganic chemistry, (2) explicit treatment of lesser reactive paraffins,  
243 (3) revised parameterization for reactive paraffin, olefin, and aromatic reactions, (4) inclusion of  
244 alkyl and acyl peroxy radical interactions and their reaction with NO<sub>3</sub>, (5) inclusion of organic  
245 nitrates and hydroperoxides, and (6) refined isoprene chemistry. Although intercomparison  
246 including CBM-Z has not been reported, the overall photochemical reactivity would be assumed  
247 to be similar to CBM-V, which gives higher and lower O<sub>3</sub> than CBM-IV and SAPRC99,  
248 respectively. Thus, maximum values of daytime net O<sub>3</sub> production of CMAQ 5.0.2 and 4.7.1 in  
249 July are ca.10 and 7-9 ppbv hr<sup>-1</sup> as compared to ca. 6 and ca. 2 ppbv hr<sup>-1</sup> by NAQM in Beijing  
250 and Tokyo, respectively, showing the substantially larger values for CMAQ than NAQM. It can  
251 be noted that net O<sub>3</sub> production of NAQM shows a second peak in early morning after breaking  
252 of dawn in both Beijing and Tokyo in July, which would be a cause of overestimate of O<sub>3</sub> in the  
253 morning by NAQM simulation as seen in Fig. 2(b) and Fig. 3(b). The cause of the early  
254 morning peak of net O<sub>3</sub> production in NAQM might be due to the photolysis of higher HONO  
255 that is produced by the heterogeneous reaction of NO<sub>2</sub>, although it has not been quantified in the  
256 present study.

Fig. 5

257 In April, net chemical production of O<sub>3</sub> is in general negative for all the models both in  
258 Beijing and Tokyo except for CMAQ 4.7.1 around midday and NAQM in early morning  
259 showing slight positive values. Tendency of higher net O<sub>3</sub> production is seen particularly for  
260 CMAQ 4.7.1, which may be the main cause of higher O<sub>3</sub> by this model both in Beijing and



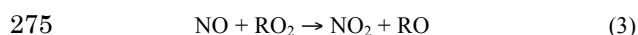
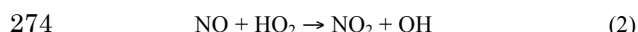


261 Tokyo in April as seen in Fig. 2(a) and Fig. 3(a). The daytime net O<sub>3</sub> production of CMAQ  
262 5.0.2 is similar to CMAQ 4.7.1 in July, but is substantially lower in April. Since the chemistry  
263 mechanism of SAPRC99 is used in common to the both CMAQ, the difference may be related  
264 to the vertical transport of some relevant species.

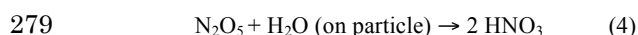
### 265 Effect of heterogeneous “renoxification” reaction of HNO<sub>3</sub>

266 Figures 2 and 3 show the common feature of anti-correlation of concentrations of O<sub>3</sub> and  
267 NO as noted above. This feature is most clearly seen for the comparison of concentrations of O<sub>3</sub>  
268 and NO in July in both cities demonstrating the large overestimate of O<sub>3</sub> and large  
269 underestimate of NO by CMAQ 4.7.1 and 5.0.2, while the much lower O<sub>3</sub> and much higher NO  
270 are estimated by NAQM. The situation in April also supports this contention.

271 It should be noted that rate constants of the most sensitive gas-phase reactions affecting the  
272 balance of O<sub>3</sub> and NO (Finlayson-Pitts and Pitts, 2000; Akimoto, 2016) such as,



276 have been well established (Burkholder et al., 2015 and earlier evaluations of the series) and  
277 more or less the same reaction rates are employed in both of SAPRC99 and CBM-Z. As for the  
278 heterogeneous processes affecting NO<sub>x</sub>, the reaction,



280 is included in common in the heterogeneous inorganic chemistry sub-module, ISORROPIA and  
281 employed in the CMAQ and NAQM models.

282 It has been noted that the simulated gaseous HNO<sub>3</sub> concentration and HNO<sub>3</sub>/NO<sub>x</sub> ratio by  
283 use of global and regional chemical transport models were found to be 2-10 times higher than  
284 the observational data during the PEM-West (Singh et al., 1996), TRACE-P (Talbot et al.,  
285 2003), and PEM-Tropics A and SONEX (Brunner et al., 2005) aircraft campaigns over the  
286 Pacific and Atlantic Ocean. It has also been reported by the ground observations in the remote  
287 troposphere at Mauna Loa (Hauglustaine et al., 1996) and in the polluted boundary layer of  
288 Beijing-Tianjin-Hebei region (Li, Y. et al., 2015).

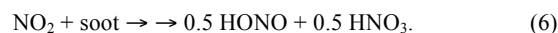
289 Another concern on recent NO<sub>x</sub> chemistry has been focused on the high concentration of  
290 HONO in the urban atmosphere, which is thought to be produced by heterogeneous reaction of  
291 NO<sub>2</sub> and H<sub>2</sub>O on the aerosol and ground surface (for example, Li, Y. et al., 2011; Gonçalves et  
292 al., 2012; Wong et al., 2013). Inclusion of the additional heterogeneous source of HONO not



only affects the photochemical  $O_3$  formation due to the increase of OH radicals but also increase  $HNO_3$  due to the increase of the reaction,  $OH + NO_2 + M \rightarrow HNO_3 + M$ . Li, Y. et al. (2015) has shown that the inclusion of heterogeneous formation of HONO gives more  $HNO_3$ , which tends to give more overestimate of gaseous  $HNO_3$  in Beijing-Tianjin-Hebei region.

In order to solve the problem of overestimation of  $HNO_3$ , heterogeneous reaction of  $HNO_3$  on soot to reproduce NO and  $NO_2$  has been proposed as “renoxification” process early by Lary et al. (1997) in the analysis of the above aircraft observation data. The heterogeneous reaction of  $HNO_3$  on soot to produce NO/ $NO_2$  has been confirmed experimentally in the laboratory studies (Disselkamp et al., 2000; Muñoz and Rossi, 2002), although the product ratio and reaction mechanism has not been well established yet. The steady state uptake coefficient  $\gamma_{ss}$  of this reaction has been reported to be  $(4.6 \pm 1.6) \times 10^{-3}$  for black soot using geometric surface area (Muñoz and Rossi, 2002).

Only NAQM among the three models studied here incorporates the following heterogeneous non-stoichiometric reactions on soot (Li, J. et al., 2015).



with  $\gamma_{HNO_3} = 3.0 \times 10^{-3}$  for Reaction (5) and  $\gamma_{HONO} = 1.0 \times 10^{-4}$  for Reaction (6). The “renoxification” by Reaction (5) would have contributed to the increase of NO in Figs. 2(c) and (d) and Figs. 3(c) and (d) to give better agreement with observation. The increase of NO could decrease  $O_3$  by the titration reaction (Reaction (1)), which may also give better agreement for  $O_3$  with the observation particularly during the nighttime. However, quantitative sensitivity analysis has not been made in the present study, and it is highly recommended that the verification of the importance of such heterogeneous renoxification reaction in model simulation against accurate measurement of gaseous  $HNO_3$  together with other  $NO_y$  in the polluted urban atmosphere.

### Effect of Vertical Transport

Other than the difference in chemical reaction mechanisms, the difference in transport module could give difference in the output of  $O_3$  concentrations. In order to analyze the effect of transport, process analysis of horizontal and vertical transport of  $O_3$  has been made for the three models. Since the horizontal transport has been found to be nearly the same for the three models, only the vertical transport will be discussed here for discussion.



Figures 6(a) and (b) shows the comparison of vertical transport of  $O_3$  among the three models in Beijing in April and July, respectively, and Figs. 6(c) and (d) shows the similar plots for Tokyo. The daytime downward vertical flux of  $O_3$  for both CMAQ models in Beijing are nearly the same ( $22\text{--}25\text{ ppbv hr}^{-1}$ ) in July, which is much larger than the values (ca.  $6\text{ ppbv hr}^{-1}$ ) in April. In contrast, those values of NAQM are ca.  $10\text{ ppbv hr}^{-1}$  both in April and July, which is larger than CMAQ in April, but smaller than CMAQ by a factor of two in July. The diurnal variation of vertical flux of  $O_3$  in Tokyo is quite different from in Beijing in July; downward  $O_3$  flux is positive only in the morning till noon and nearly zero or negative in the afternoon. Such characteristics is in common for the three models. The maximum downward fluxes of  $O_3$  in the morning in Tokyo for the CMAQ 5.0.2 (ca.  $17\text{ ppbv hr}^{-1}$ ) and CMAQ 4.7.1 (ca.  $13\text{ ppbv hr}^{-1}$ ) are much higher than for NAQM ( $< 5\text{ ppbv hr}^{-1}$ ). Thus, it would be concluded that at least a part of much higher  $O_3$  concentrations by CMAQ 5.0.2 and 4.7.1 as compared to NAQM shown Fig. 2(b) and Fig. 3(b) in Beijing and Tokyo in July can be ascribed to the higher downward flux of  $O_3$  by the CMAQ models than NAQM.

Fig. 6

Peculiar feature of vertical flux of  $O_3$  shown in Fig. 6 is the strong positive morning peak at around 7 and 6 am for CMAQ 5.0.2 particularly in Beijing in April and July, respectively, and also at 6–7 am in Tokyo in April. Another point to be noted is the delayed rise of vertical downward flux of  $O_3$  by nearly 2 hours for NAQM both in April and July and in Beijing and Tokyo. Although this feature is not scrutinized in this study, it should be reminded here that the vertical transport module affects significantly the simulated results of  $O_3$  in regional chemical transport models.

#### Comparison of Transport Process for CMAQ v. 5.0.2 and v. 4.7.1

As seen in Fig. 2 and Fig. 3, CMAQ 5.0.2 gives relatively low  $O_3$  and relatively high NO mixing ratios closer to NAQM in April, but relatively high  $O_3$  and low NO closer to CMAQ 4.7.1 in July both in Beijing and Tokyo. Since the chemical mechanisms of CMAQ 5.0.2 and CMAQ 4.7.1 are the same, the difference in the model performance must be ascribed to the difference in transport processes. Figures 7(a) and (b) show the comparison of mixing ratios of  $O_3$  and hourly  $O_3$  mixing ratios change between CMAQ 5.0.2 and observation in Beijing in April and the similar plots in July are shown in Figs. 7(c) and (d), respectively. As for the observational values, the data provided by IAP are used for the plots. The large rise of  $O_3$  concentration change at 7–8 am shown in Figs. 7(b) and (d) clearly correspond to the early morning peak of downward transport flux of  $O_3$  at 6–7 am as seen in Figs. 6(a) and (b). Such a

Fig. 7



sharp rise at 7 am is not seen for CMAQ 4.7.1 although a small peak is discernable in April. This implies that such a feature is due to the characteristics of the vertical transport module of CMAQ 5.0.2. The similar plots for NO are shown in Figs. 8(a)-(d). In April, NO mixing ratio by CMAQ 5.0.2 rises in early morning, which corresponds well with the observation. The cause of such an early morning rise of NO mixing ratio and hourly mixing ratio change would be due to the increase of traffic in the morning. In July however, although the observation of NO mixing ratio and hourly change shows similar morning peak in April, CMAQ 5.0.2 simulation doesn't give any such morning peak, which would correspond to very low mixing ratio of NO simulated by CMAQ 5.0.2 together with CMAQ 4.7.1 as seen in Fig. 2(d). Although the phenomena could be caused by rapid oxidation of NO to NO<sub>2</sub> in summer, the reason is unknown at this stage.

Fig. 8

It should be noted that after the large rise at 7-8 am, the hourly change of O<sub>3</sub> mixing ratio by CMAQ 5.0.2 agrees well with the observed O<sub>3</sub> change in late morning and afternoon as shown in Fig 7(b) and (d). This implies that the large morning surge give much earlier rise of O<sub>3</sub> compared to observation. It can be noted, however, the morning surge at 7 am in July is ca. 15 ppbv, which is not very much higher than ca.10 ppbv in April. Thus, although the morning surge is larger in July than in April, this would not be the main cause of the much higher predicted O<sub>3</sub> concentration in the morning in July as compared to in April. The large difference in the simulated concentration of nighttime O<sub>3</sub> can be seen between April and July for CMAQ 5.0.2, and also between CMAQ 5.0.2 and CMAQ 4.7.1 in April. The nighttime O<sub>3</sub> is as low as 10-20 ppbv in Beijing, and 20-30 ppbv in Tokyo both for CMAQ 5.0.2 and NAQM in April agreeing with observation. However, the nighttime O<sub>3</sub> by CMAQ 4.7.1 is as high as 30 and 45 ppbv in April in Beijing and Tokyo, respectively. In July, the nighttime O<sub>3</sub> is 20-30 ppbv in Beijing and ca. 20 ppbv in Tokyo by NAQM, which are closer to the observation, while both CMAQ models give 40-50 ppbv both in Beijing and Tokyo, which is substantially higher than observation. The high nighttime O<sub>3</sub> by CMAQ models would contribute at least partly to the daytime high O<sub>3</sub> in July. Although coarse resolution of 45 km grid may tends to give the higher nighttime O<sub>3</sub> due to less effective NO titration, it would not enough to explain such high nighttime O<sub>3</sub> by CMAQ 4.7.1 both for April and July, and CMAQ 5.0.2 for July since NAQM with the same grid size reproduce the nighttime O<sub>3</sub> as low as 20 ppb, agreeing better with observation. It would be important to quantify the effect of the heterogeneous production of nighttime NO from HNO<sub>3</sub> to evaluate its impact on nighttime O<sub>3</sub>.



### Comparison with the observational data of O<sub>3</sub> in Beijing and Tokyo

Both CMAQ 5.0.2 and NAQM give reasonably good agreement of O<sub>3</sub> mixing ratios in April in Tokyo. It can be noted that both of CMAQ 5.0.2 and NAQM gives higher mixing ratio by 10-15 ppb after the dawn. For CMAQ 5.0.2, as mentioned above, the overestimate would be caused by the peak of downward flux of O<sub>3</sub> in early morning. NAQM gives similar overestimate of O<sub>3</sub> mixing ratio by ca. 10 ppbv in early morning, but this phenomenon would be caused by peak of net chemical ozone production (Fig. 5) rather than the vertical transport. Although the cause of the early morning peak of the net O<sub>3</sub> production has not been elucidated in this study, it may be related to the photolysis of HONO accumulated during nighttime, since heterogeneous production of HONO (Eq. 6) is included in NAQM.

In July, NAQM is the sole model giving good agreement with observation in Tokyo. It can be noted, however, that the calculated concentration is higher than observation by ca. 10 ppbv in early morning similar to April. Such higher rise of O<sub>3</sub> mixing ratio in early morning is discernible in July in Tokyo for CMAQ 5.0.2. The same phenomenon can also be seen in July in Tokyo, and the cause would be due the early morning peaks of downward flux and net ozone production for CMAQ5.0.2 and NAQM, respectively. It should be noted that the enhanced mixing ratios of O<sub>3</sub> in early morning are persistent at least till noon giving the higher values of simulated mixing ratios.

Substantially higher simulated O<sub>3</sub> mixing ratios than observation by CMAQ 4.7.1 both in April and July, and by CMAQ 5.0.2 in July in Tokyo (Figs. 3(a) and (b)), may at least partially be caused by the higher nighttime mixing ratios of O<sub>3</sub>, which would contribute to the baseline mixing ratio for the whole day. It would be expected that if the nighttime O<sub>3</sub> can be reduced to the observational level, better agreement of O<sub>3</sub> with observation would be expected for the whole day.

As for the observational data in Beijing, the daily maximum of O<sub>3</sub> mixing ratio in July is ca. 90 ppbv by Xu et al. (2011) and ca. 60 ppbv by the IAP data, while nighttime minimum are both 10-20 ppbv consistently. Since maximum O<sub>3</sub> mixing ratio in summer is expected to be higher in Beijing than in Tokyo (ca. 60 ppbv) due to the higher NO (see Figs. 2(d) and 3(d)) and NO<sub>2</sub> (not shown) levels by a factor of ~2, the higher observational data than in Tokyo in Fig. 2(c) could be more representative for the average of the calculated grids in Beijing. Although there still is large uncertainty as for the monthly averaged observational data of O<sub>3</sub> in Beijing in 2010, the tendency of the overestimate by CMAQ 5.0.2 and 4.7.1, and the underestimation of NAQM in Beijing in July could be suggested.



In April in Beijing, Chen et al. (2016) reported the daily maximum mixing ratio of  $O_3$  at ca. 65 ppbv in 2015, which is substantially higher than the IAP data of ca. 40 ppbv in 2010. Meanwhile, the surface ozone increase has been reported in Beijing at the rural sites of Shangdianzi in the period of 2004–2015 with regard to the maximum daily average 8 hr mixing ratios (MDA8) (Ma et al., 2016). Although the long-term increasing trend indicates an average rate of  $1.13 \pm 0.01$  ppb  $yr^{-1}$ , no monthly data was reported and the year-by-year variability would be substantial. If we assume the monthly averaged MDA8 values in April in 2010 is lower than 2015 by 10 ppbv, the uncertainty of the daily maximum observational value in April in Beijing would be in the range of 40–55 ppbv. Thus, within the uncertainty range, the tendency of overestimation of CMAQ 4.7.1, and the underestimation by NAQM could be suggested.

As for the discussion of reproducibility of the model simulation for observational data, comparison for three-year averaged values in more recent years after 2013, when the routine monitoring data at much more number of sites within the targeted grids are available, would be highly desirable particularly in Beijing.

#### **Overestimate of $O_3$ at Oki, a remote oceanic site**

At the remote site of Oki, overestimate of ca. 20 ppb for daytime  $O_3$  has been seen in July in Fig. 4(b) for all the three models with spatial resolution of 45 km. Such overestimate of summertime  $O_3$  at Oki by CMAQ models has been reported by Lin et al. (2009) with MM5-CMAQ v. 4.6 (27 km  $\times$  27 km), while much better agreement with observation is also reported previously by Yamaji et al. (2006) (80 km  $\times$  80 km) with RAMS-CMAQ v. 4.4, and Li, J. et al. (2007) with NAQM (81 km  $\times$  81 km). The seasonal variation of  $O_3$  at remote sites around Japan has been known well showing springtime monthly maximum of ca. 60 ppb and summertime monthly minimum of 35–40 ppb (Pochanart et al., 1999, 2002), which is consistent with the observational data shown in Fig. 4. The summertime minimum at Oki and other remote islands in this region are well established to be due to prevailing clean marine air in this area (Pochanart et al., 2002; Yamaji et al., 2006).

Since the overestimate does not depend on the spatial resolution of the model, and daytime buildup of  $O_3$  due to local photochemical activity is <10 ppbv by the observation and 5–15 ppbv by the simulation as shown in Fig. 4(b), the overestimate of  $O_3$  concentration in July by all the three models cannot be ascribed to the direct influence of nearby terrestrial emissions of precursors in mainland Japan due to the low spatial resolution of the models. Overestimate



could be either due to more frequent influence of terrestrial air mass by WRF compared to the real meteorology or higher O<sub>3</sub> concentration in the oceanic air around this area affected by the influence of non-episodic terrestrial emissions including long-range transport. The reproduction of observed concentration by models at Oki would be important for the analysis of air quality in Japan since air mass passing through Oki provides a flowing-in background mixing ratio to the mainland of Japan.

#### Summary

In order to identify substantial variability among the simulated modelling results for surface ozone in MICS-Asia III even though using the same emission, meteorological field and boundary conditions, three regional models, CMAQ 5.0.2, 4.7.1 and NAQM were selected and the detailed comparison have been made in the selected grids covering metropolitan areas in Beijing and Tokyo and at a remote oceanic site of Oki. The analyses were made for the monthly averaged diurnal change of surface ozone in April and July in 2010.

The simulated O<sub>3</sub> concentration was the highest for CMAQ 4.7.1 followed by CMAQ 5.0.2 and NAQM both in Beijing and Tokyo in April, while both CMAQ models gave similar values of O<sub>3</sub> but much higher than NAQM in July. At Oki, simulation for O<sub>3</sub> by all the three models agrees well each other and with observation in April. In July, however, all the models overestimated daytime O<sub>3</sub> by ca. 20 ppb compared to observation.

Three causes of resulting the difference among model outputs have been identified and discussed.

- (1) The chemistry mechanism sub-module, SAPRC99 used in the CMAQ was found to give higher net ozone production than CBM-Z in NAQM agreeing with previous studies.
- (2) Higher NO concentration have been predicted by NAQM than CMAQ possibly due to the inclusion of heterogeneous “renoxification” reaction of HNO<sub>3</sub> (on soot) → NO + NO<sub>2</sub> giving better agreement with observational concentration particularly for nighttime NO and O<sub>3</sub>.
- (3) Vertical downward flux of O<sub>3</sub> was found to affect substantially the diurnal pattern and mixing ratios of O<sub>3</sub>. The large difference in the performance of O<sub>3</sub> in April and July of CMAQ 5.0.2 would also have been due to the difference in downward flux caused by the difference of meteorological conditions.





## 486 Acknowledgements

487 This work was supported by the Global Environmental Research Fund (S-12) by Ministry  
488 of Environment, Japan, and Natural Science Foundation of China (41620104008).

## 490 References

- 491 Akimoto, H., *Atmospheric Reaction Chemistry*, Springer Japan, Tokyo, 2016.
- 492 Binkowski, F. S. and S. J. Roselle<sup>1</sup>, Models-3 Community Multiscale Air Quality(CMAQ)  
493 model aerosol component 1. Model description, J. Geophys. Res., 108, D6, 4183,  
494 doi:10.1029/2001JD001409, 2003.
- 495 Brunner, D., J. Staehelin, H. L. Rogers, M. O. Köhler, J. A. Pyle, D. A. Hauglustaine, L.  
496 Jourdain, T. K. Berntsen, M. Gauss, I. S. A. Isaksen, E. Meijer, P. van Velthoven, G. Pitari,  
497 E. Mancini, V. Grewe, and R. Sausen, An evaluation of the performance of chemistry  
498 transport models – Part 2: Detailed comparison with two selected campaigns, Atmos. Chem.  
499 Phys., 5, 107–129, 2005.
- 500 Burkholder, J. B., S. P. Sander, J. P. D. Abatt, J. R. Barker, R. E. Huie, C. E. Kolb, M. J. Kurylo,  
501 V. L. Orkin, D. M. Wilmouth, and P. H. Wine, Chemical Kinetics and Photochemical Data  
502 for Use in Atmospheric Studies, Evaluation Number 18, JPL Publication 15-10, Pasadena,  
503 California, <http://jpldataeval.jpl.nasa.gov/>, 2015.
- 504 Carter, W. L., Implementation of the SAPRC-99 chemical mechanism into the Models-3  
505 framework, Report to the United States Environmental Protection Agency, January 29, 2000.
- 506 Chen, W., H. Tang, and H. Zhao, Diurnal, weekly and monthly spatial variations of air  
507 pollutants and air quality of Beijing, Atmos. Environ., 119, 21-34, 2015.
- 508 CMAS, Operational Guidance for the Community Multiscale Air Quality (CMAQ) Modeling  
509 System: Version 5.0, [https://www.airqualitymodeling.org/index.php/CMAQ\\_version\\_5.0\\_](https://www.airqualitymodeling.org/index.php/CMAQ_version_5.0_)  
510 (February\_2010\_release)\_OGD, 2011.
- 511 Disselkamp, R. S., M. A. Carpenter, J. P. Cowin, A chamber investigation of nitric acid-soot  
512 aerosol chemistry at 298 K, J. Atmos. Chem., 37, 113-123, 2000.
- 513 Faraji, M., Y. Kimura, and D. Allen, Comparison of the Carbon Bond and SAPRC  
514 photochemical mechanisms under conditions relevant to southeast Texas, Atmos. Environ.,  
515 42, 5821-5836, 2007.
- 516 Finlayson-Pitts, B. J. and J. N. Pitts, Jr., *Chemistry of the Upper and Lower Atmosphere*,  
517 Academic Press, 2000.
- 518 Fiore, A. M. et al. (46 other co-authors), Multimodel estimates of intercontinental source-



- 519 receptor relationships for ozone pollution, *J. Geophys. Res.*, 114, D04301,  
520 doi:10.1029/2008JD010816, 2009.
- 521 Foley, K. M., S. J. Roselle, K. W. Appel, P. V. Bhawe, J. E. Pleim, T. L. Otte, R. Mathur, G.  
522 Sarwar, J. O. Young, R. C. Gilliam, C. G. Nolte, J. T. Kelly, A. B. Gilliland, and J. O. Bash,  
523 Incremental testing of the Community Multiscale Air Quality (CMAQ) modeling system  
524 version 4.7, *Geosci. Model Dev.*, 3, 205–226, 2010.
- 525 Fountoukis, C. and A. Nenes, ISORROPIA II: a computationally efficient thermodynamic  
526 equilibrium model for  $K^+$ – $Ca^{2+}$ – $Mg^{2+}$ – $NH_4^+$ – $Na^+$ – $SO_4^{2-}$ – $NO_3^-$ – $Cl^-$ – $H_2O$  aerosols,  
527 *Atmos. Chem. Phys.*, 7, 4639–4659, 2007.
- 528 Fu, J. S., X. Dong, Y. Gao, D. C. Wong, and Y. F. Lam, Sensitivity and linearity analysis of  
529 ozone in East Asia: The effects of domestic emission and intercontinental transport, *J. Air  
530 Waste Manag. Assoc.*, 62, 1102–1114, 2012.
- 531 Gery, M. W., G. Z. Whitten, J. P. Killus, and M. C. Dodge, A photochemical kinetics  
532 mechanism for urban and regional scale computer modeling, *J. Geophys. Res.*, 94,  
533 12,925–12,956, , 1989.
- 534 Gonçalves, M., D. Dabdub, W. L. Chang, O. Jorba, and J. M. Baldasano, Impact of HONO  
535 sources on the performance of mesoscale air quality models, *Atmos. Environ.*, 54, 168–176,  
536 2012.
- 537 Han, Z., T. Sakurai, H. Ueda, G. R. Carmichael, D. Streets, H. Hayami, Z. Wang, T. Holloway,  
538 M. Engardt, Y. Hozumi, S. U. Park, M. Kajino, K. Sartelet, C. Fung, C. Bennet, N.  
539 Thongboonchoo, Y. Tang, A. Chang, K. Matsuda, M. Amann, MICS-Asia II: Model  
540 intercomparison and evaluation of ozone and relevant species, *Atmos. Environ.* 42, 3491–  
541 3509, 2008.
- 542 Hauglustaine, D. A., B. A. Ridley, S. Solomon, P. G. Hess, S. Madronich,  $HNO_3/NO_x$  ratio in  
543 the remote troposphere During MLOPEX 2: Evidence for nitric acid reduction on  
544 carbonaceous aerosols?, *Geophys Res. Lett.*, 23, 2609–2612, 1996.
- 545 Jaffe, D. A., R. E. Honrath, L. Zhang, H. Akimoto, A. Shimizu, H. Mukai, K. Murano, S.  
546 Hatakeyama, and J. Merrill, Measurements of  $NO$ ,  $NO_y$ ,  $CO$  and  $O_3$  and estimation of the  
547 ozone production rate at Oki Island, Japan, during PEM-West, *J. Geophys. Res.*, 101,  
548 2037–2048, 1996.
- 549 Jimenez, P., Jose M. Baldasano, and D. Dabdub, Comparison of photochemical mechanisms for  
550 air quality modeling, *Atmos. Environ.*, 37, 4179–4194, 2003.
- 551 Kurokawa, K., T. Ohara, I. Uno, M. Hayasaka, and H. Tanimoto, Influence of meteorological



- 552 variability on interannual variations of springtime boundary layer ozone over Japan during  
553 1981–2005, *Atmos. Chem. Phys.*, 9, 6287–6304, 2009.
- 554 Lary, D. J., A.M. Lee, R. Toumi, M. J. Newchurch, M. Pirre, and J. B. Renard, Carbon aerosols  
555 and atmospheric photochemistry, *J. Geophys. Res.*, 102, 3671–3682, 1997.
- 556 Li, J., Z. Wang, H. Akimoto, C. Gao, P. Pochanart, and X. Wang, Modeling study of ozone  
557 seasonal cycle in lower troposphere over east Asia, *J. Geophys. Res.*, 112, D22S25,  
558 doi:10.1029/2006JD008209, 2007.
- 559 Li, J., H. Dong, L. Zeng, Y. Zhang, M. Shao, Z. Wang, Y. Sun, and P. Fu, Exploring possible  
560 missing sinks of nitrate and its precursors in current air quality models—A case simulation  
561 in the Pearl River Delta, China, using an observation-based box model, *SOLA*, 11, 124–128,  
562 2015.
- 563 Li, J., Z. Wang, G. Zhuang, G. Luo, Y. Sun, and Q. Wang, Mixing of Asian mineral dust with  
564 anthropogenic pollutants over East Asia: a model case study of a super-duststorm in March  
565 2010, *Atmos. Chem. Phys.*, 12, 7591–7607, 2012.
- 566 Li, J., T. Nagashima, et al., in this special issue to be published.
- 567 Li, M., Zhang, Q., Kurokawa, J., Woo, J.-H., He, K. B., Lu, Z., Ohara, T., Song, Y., Streets, D.  
568 G., Carmichael, G. R., Cheng, Y. F., Hong, C. P., Huo, H., Jiang, X. J., Kang, S. C., Liu, F.,  
569 Su, H., and Zheng, B., MIX: a mosaic Asian anthropogenic emission inventory for the  
570 MICS-Asia and the HTAP projects, *Atmos. Chem. Phys.* 17, 935–963, 2017.
- 571 Li, Y., J. An, M. Min, W. Zhang, F. Wang, and P. Xie, Impacts of HONO sources on the air  
572 quality in Beijing, Tianjin and Hebei Province of China, *Atmos. Environ.*, 45, 4735–4744,  
573 2011.
- 574 Li, Y., J. An, M. Kajino, J. Li, and Y. Qu, Impacts of additional HONO Sources on  
575 concentrations and deposition of NO<sub>y</sub> in the Beijing-Tianjin-Hebei Region of China,  
576 *SOLA*, 11, 36–42, 2015.
- 577 Lin, M., T. Holloway, T. Oki, D. G. Streets, and A. Richter, Multi-scale model analysis of  
578 boundary layer ozone over East Asia, *Atmos. Chem. Phys.*, 9, 3277–3301, 2009.
- 579 Luecken, D. L., S. Phillips, G. Sarwar and C. Jang, Effects of using the CB05 vs. SAPRC99 vs.  
580 CB4 chemical mechanism on model predictions: Ozone and gas-phase photochemical  
581 precursor concentrations, *Atmos. Environ.*, 42, 5805–5820, 2008.
- 582 Ma, Z., J. Xu, W. Quan, Z. Zhang, W. Lin, and X. Xu, Significant increase of surface ozone at a  
583 rural site, north of eastern China, *Atmos. Chem. Phys.*, 16, 3969–3977, 2016.
- 584 Monks, P. S., A review of the observations and origins of the spring ozone maximum, *Atmos.*



- 585 Environ., 34, 3545–3561, 2000.
- 586 Muñoz, M. S. S. and M. J. Rossi, Heterogeneous reactions of  $\text{HNO}_3$  with flame soot generated
- 587 under different combustion conditions. Reaction mechanism and kinetics, Phys. Chem.
- 588 Chem. Phys., 4, 5110–5118, 2002.
- 589 Nenes, A., S. N. Pandis, and C. Pilinis, ISORROPIA: A new thermodynamic equilibrium model
- 590 for multiphase multicomponent inorganic, Aerosols, Aquat. Geochem., 4, 123–152, 1998.
- 591 Pleim, J. E., A combined local and nonlocal closure model for the atmospheric boundary layer.
- 592 Part I: Model description and testing, J. Appl. Meteor. Climatol., 46, 1383–1395, 2007.
- 593 Pochanart, P., J. Hirokawa, Y. Kajii, and H. Akimoto, Influence of regional-scale anthropogenic
- 594 activity in northeast Asia observed at Oki, Japan, J. Geophys. Res., 104, 3621–3631, 1999.
- 595 Pochanart, P., H. Akimoto, Y. Kinjo, H. Tanimoto, Surface ozone at four remote island sites
- 596 and the preliminary assessment of the exceedances of its critical level in Japan, Atmos.
- 597 Environ., 36, 4235–4250, 2002.
- 598 Pochanart, P., H. Akimoto, Y. Kajii, V. M. Potemkin, and T. V. Khodzher, Regional
- 599 background ozone and carbon monoxide variations in remote Siberia/East Asia, J. Geophys.
- 600 Res., 108, 4028, doi:10.1029/2001JD001412, 2003.
- 601 Sarwar, G., D. Luecken, G. Yarwood, G. Whitten, and W. P. L. Carter, Impact of an updated
- 602 Carbon Bond mechanism on predictions from the CMAQ modeling system: preliminary
- 603 assessment, J. Appl. Meteor. Climat. 47, 3–14, 2008.
- 604 Singh, H. B., D. Herlth, R. Kolyer, L. Salas, J. D. Bradshaw, S. T. Sandholm, D. D. Davis J.
- 605 Crawford, Y. Kondo, M. Koike, R. Talbot, G. L. Gregory, G. W. Sachse, E. Browell, D. R.
- 606 Blake, F. S. Rowland, R. Newell, J. Merrill, B. Heikes, S. C. Liu, P. J. Crutzen, M.
- 607 Kanakidou, Reactive nitrogen and ozone over the western Pacific: Distribution, partitioning,
- 608 and sources, J. Geophys Res., 101, 1793–1808, 1996.
- 609 Talbot, R., J. Dibb, E. Scheuer, G. Seid, R. Russo, S. Sandholm, D. Tan, H. Singh, D. Blake, N.
- 610 Blake, E. Atlas, G. Sachse, C. Jordan, M. Avery, Reactive nitrogen in Asian continental
- 611 outflow over the western Pacific: Results from the NASA Transport and Chemical Evolution
- 612 over the Pacific (TRACE-P) airborne mission, J. Geophys Res., 108, D20,
- 613 doi: 10.1029/2002JD003129, 2003.
- 614 Walcek, C. J. and N. M. Aleksic, A simple but accurate mass conservative, peak-preserving,
- 615 mixing ratio bounded advection algorithm with FORTRAN code, Atmos. Environ., 32,
- 616 3863–3880, 1998.
- 617 Wang, Z. F., et al. overview paper, in this special issue to be published.



- 618 Wong, K. W., C. Tsai, B. Lefer, N. Grossberg, and J. Stutz, Modeling of daytime HONO  
619 vertical gradients during SHARP 2009, Atmos. Chem. Phys., 13, 3587–3601, 2013.
- 620 Xu, J., J. Z. Ma, X. L. Zhang, X. B. Xu, X. F. Xu, W. L. Lin, Y. Wang, W. Meng, and Z. Q. Ma,  
621 Measurements of ozone and its precursors in Beijing during summertime: impact of urban  
622 plumes on ozone pollution in downwind rural areas, Atmos. Chem. Phys., 11, 12241–12252,  
623 2011.
- 624 Yamaji, K., T. Ohara, I. Uno, H. Tanimoto, J. Kurokawa, and H. Akimoto, Analysis of the  
625 seasonal variation of ozone in the boundary layer in East Asia using the Community  
626 Multi-scale Air Quality model: What controls surface ozone levels over Japan?, Atmos.  
627 Environ., 40, 1856–1868, 2006.
- 628 Yamaji, K., T. Ohara, I. Uno, J. Kurokawa, P. Pochanart, and H. Akimoto, Future prediction of  
629 surface ozone over east Asia using Models-3 Community Multiscale Air Quality Modeling  
630 System and Regional Emission Inventory in Asia, J. Geophys. Res., 113, D08306,  
631 doi:10.1029/2007JD008663, 2008.
- 632 Yamartino, R. J., Nonnegative, conserved scalar transport using grid-cell-centered, spectrally  
633 constrained Blackman cubics for applications on a variable-thickness mesh, Mon. Weather  
634 Rev. 121, 753–763, 1993.
- 635 Zaveri, R. A. and L. K. Peters, A new lumped structure photochemical mechanism for  
636 large-scale applications, J. Geophys. Res., 104, 30,387–30,415, 1999.
- 637

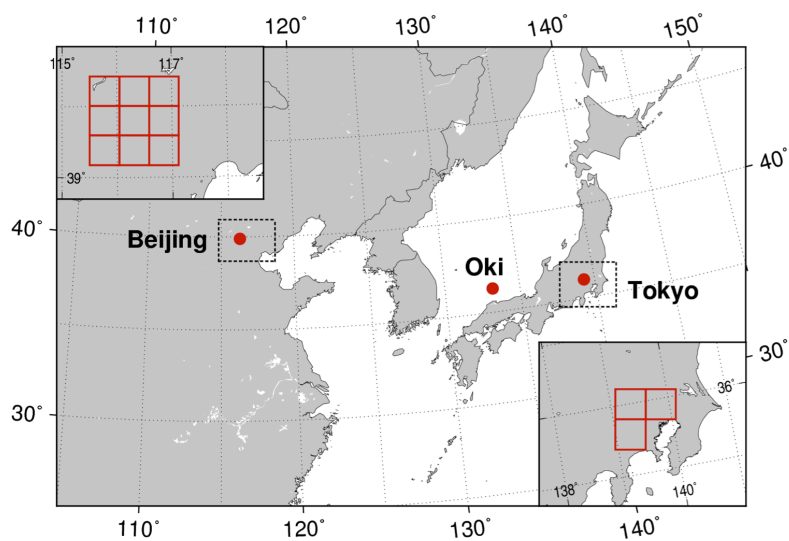


Fig. 1 Grids for comparison of the model simulation and observation; Beijing and Tokyo metropolitan area and Oki EANET site

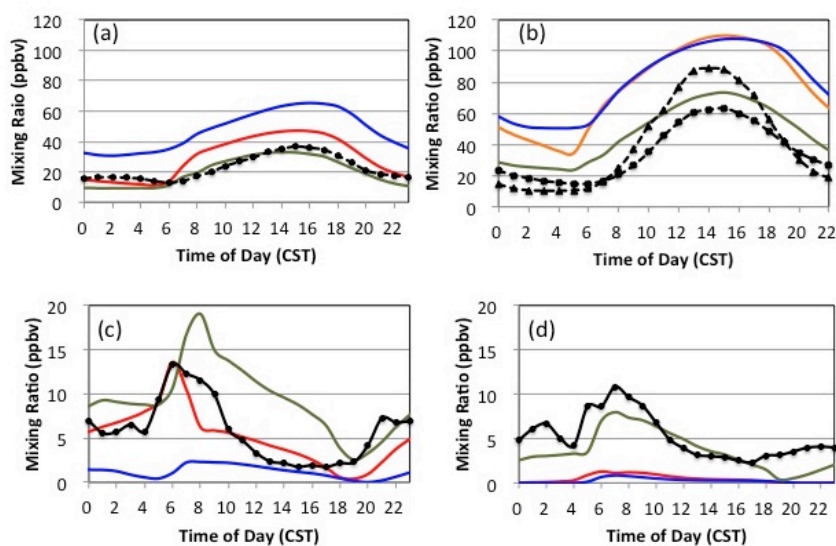


Fig. 2 Monthly averaged diurnal variation in Beijing, (a)  $O_3$  in April, (b)  $O_3$  in July, (c)  $NO$  in April, and (d)  $NO$  in July. Observation: (IAP), (Xu et al.); CMAQ 5.0.2: (red line); CMAQ 4.7.1: (blue line); NAQM: (green line)

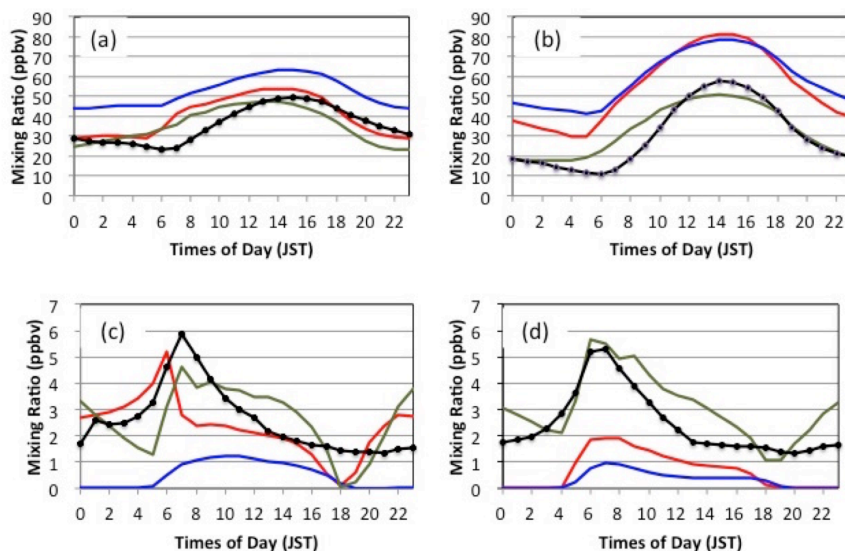


Fig. 3 Monthly averaged diurnal variation in Tokyo, (a)  $O_3$  in April, (b)  $O_3$  in July, (c) NO in April, and (d) NO in July. Observation —●—; CMAQ 5.0.2 —●—; CMAQ 4.7.1 —●—; NAQM —●—

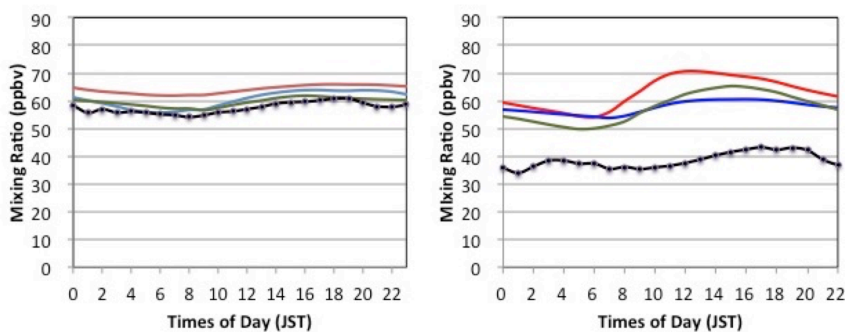


Fig. 4 Monthly averaged diurnal variation of  $O_3$  at Oki (a) in April, (b) in July. Observation —●—; CMAQ 5.0.2 —●—; CMAQ 4.7.1 —●—; NAQM —●—



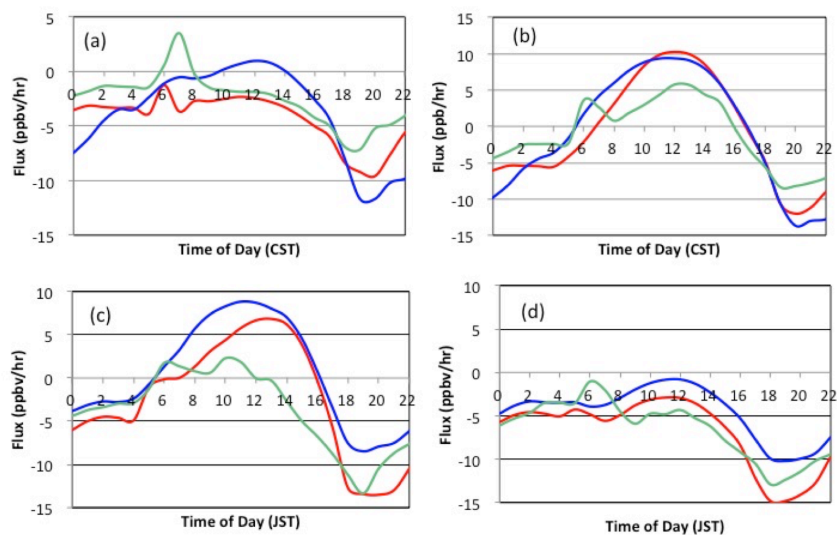


Fig. 5 Comparison of net chemical  $O_3$  production in (a) Beijing in April, (b) Beijing in July, (c) Tokyo in April, and (d) Tokyo in July. CMAQ 5.0.2 — ; CMAQ 4.7.1 — ; NAQM —

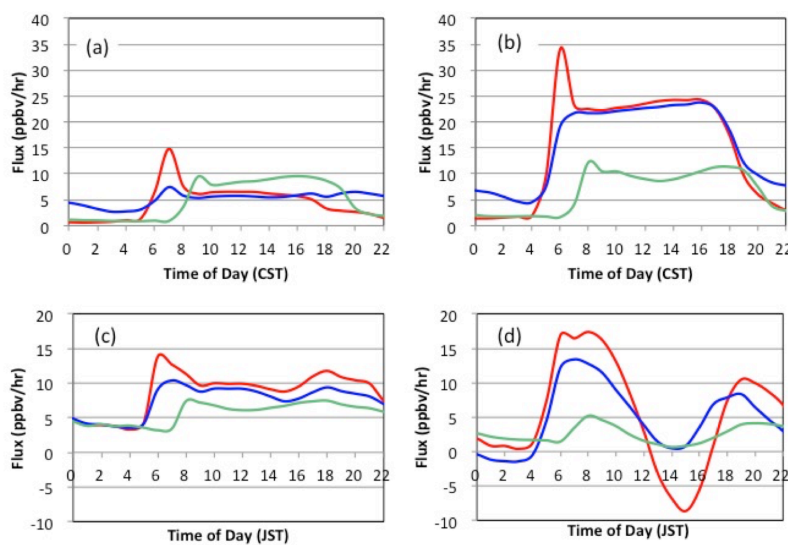


Fig. 6 Comparison of vertical transport of  $O_3$  in (a) Beijing in April, (b) Beijing in July, (c) Tokyo in April, and (d) Tokyo in July. CMAQ 5.0.2 — ; CMAQ 4.7.1 — ; NAQM —

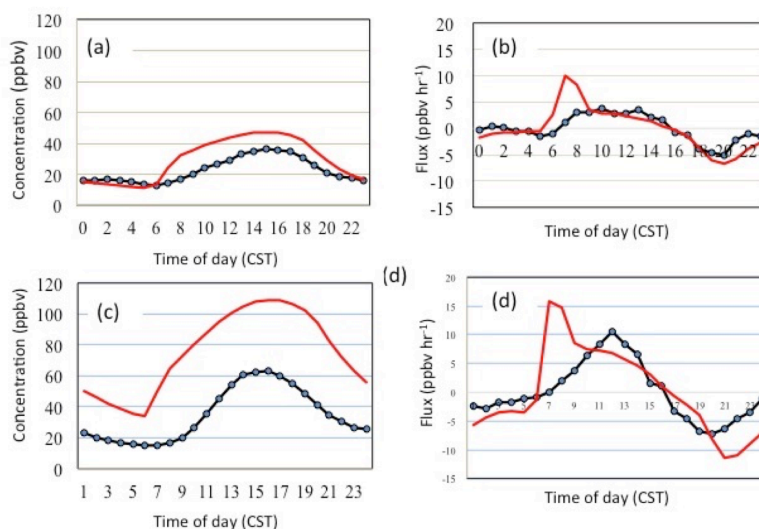


Fig. 7 Monthly averaged diurnal variation of (a)  $O_3$  concentration in April, (b) hourly  $O_3$  concentration change in April, (c)  $O_3$  concentration in July and (d) hourly  $O_3$  concentration change in July in Beijing. CMAQ 5.0.2 —, Observation —●—

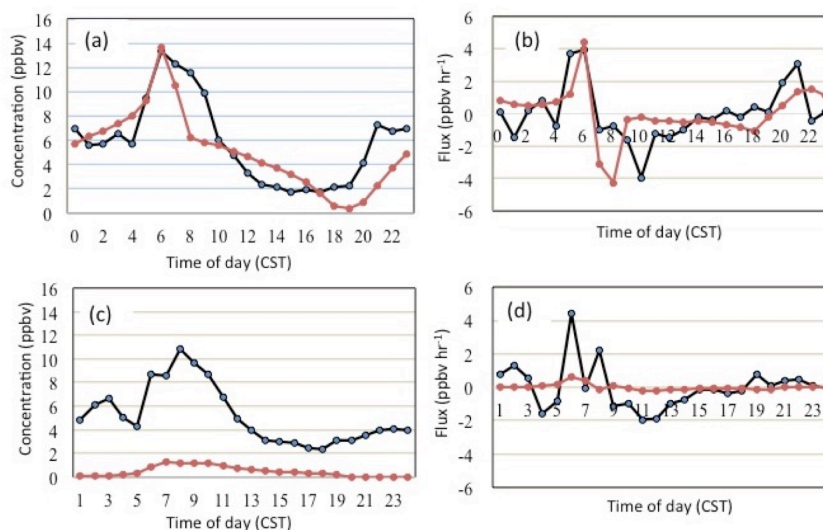


Fig. 8 Monthly averaged diurnal variation of (a) NO concentration in April, (b) hourly NO concentration change in April, (c) NO concentration in July and (d) hourly NO concentration change in July in Beijing. CMAQ 5.0.2 —, Observation —●—